Influence of the interaction range on the stability of following models

Antoine Tordeux
a.tordeux@fz-juelich.de
JSC, FZ Jülich

Mohcine Chraibi
m.chraibi@fz-juelich.de
JSC, FZ Jülich

Armin Seyfried
a.seyfried@fz-juelich.de
JSC, FZ Jülich and Wuppertal University

ABSTRACT

One proposes to analyze the stability of the uniform solutions of microscopic second order following models with $K \geq 1$ predecessors in interaction. We calculate general conditions for that the linear stability occurs, and explore the results with particular distance based pedestrian and car-following models. Non linear relations between K and the stability are established.

Categories and Subject Descriptors

G.1.7 [**Ordinary Differential Equations**]: Convergence and stability

General Terms

Linear stability theory

Keywords

Car-following model; Linear stability analysis of uniform solution; Number of predecessors in interaction

1. INTRODUCTION

Microscopic particles systems are frequently used to model pedestrian crowd or road traffic flow behaviors [3, 6]. Continuous models are defined with differential equations systems. The differential systems can be ordinary, stochastic or delayed, and of first or second order. The models have the uniform configuration (where the spacing and the speed are constant and equal) as equilibrium solution. The linear stability analysis of the uniform solutions allows to describe stationary state of the models [11]. The method consists in determining conditions on the parameters for which perturbations around the uniform solution vanish.

The number of predecessors in interaction is an essential parameter of the models. It is interpreted as an anticipation factor in traffic flow modeling [15]. Many car-following models with several predecessors in interaction exist in the literature [2, 10, 9, 12]. For pedestrian models, the parameter corresponds to the interaction range. In this paper, we calculate the linear stability for general ordinary models of second order with $K \geq 1$ predecessors in interaction. The results are explored with particular distance-based pedestrian and car-following models. They allow to justify when and why only a limited number of preceding agents needs to be taken into account when practically determining the acceleration of an agent.

1.1 Definition of the model

Let us consider an infinite 1D system of agents moving in the same direction. We denotes $n \in \mathbb{N}$ the index and (x_n) the curvilinear positions of the agents. We suppose that the initial positions are such that the predecessor of the agent n is the agent $n+1$.

The dynamics of the system are described by the second order model

$$\ddot{x}_n(t) = A\big(\dot{x}_n(t), x_{n+1}(t) - x_n(t), \dot{x}_{n+1}(t), \dots, x_{n+K}(t) - x_n(t), \dot{x}_{n+K}(t)\big). \quad (1)$$

The acceleration A of the agent n at time $t \geq 0$ depends on the speed, and on the speeds and distance spacings of the K predecessors at the same time. We assume the function A differentiable.

1.2 Uniform solution

For a given mean spacing $d > 0$, we suppose that a speed v exists such that $A(v, d, v, 2d, v, \dots, Kd, v) = 0$. Under this assumption, the uniform (or homogeneous) configurations H such that for all $t \geq 0$ and all n

$$x^H_{n+1}(t) - x^H_n(t) = d, \qquad x^H_n(t) = x^H_n(0) + vt, \quad (2)$$

are solution of the system. It exists an infinity of uniform configurations, depending on the initial conditions. The linear stability of these solutions is investigated in this paper.

2. LINEAR STABILITY ANALYSIS

The literature distinguishes local stability analysis, for a finite line of agents with a leader traveling at a know speed, and global stability, for agents on a ring or on an infinite lane. The global stability conditions are more restrictive since they contain as well convective perturbations, that can locally vanish [14]. Here the global stability conditions are calculated on an infinite lane.

2.1 Characteristic equation

The stability conditions are calculated by studying the evolution of the differences $\tilde{x}_n(t) = x_n(t) - (x^H_n(0) + vt)$. An uniform solution H is stable if $\lim_{t\to\infty} \tilde{x}_n(t) = \lim_{t\to\infty} \dot{\tilde{x}}_n(t) = 0$ for all n.

A first order Taylor approximation of (1) leads to the linear dynamics

$$\ddot{y}_n(t) = \sum_{k=1}^{K} \alpha_k (y_{n+k}(t) - y_n(t)) + \sum_{k=0}^{K} \beta_k \dot{y}_{n+k}(t). \quad (3)$$

where $\alpha_k = \frac{\partial A}{\partial d_k}(v, d, v, \ldots)$ and $\beta_k = \frac{\partial A}{\partial v_k}(v, d, v, \ldots)$.

A uniform configuration H is linearly stable if $\lim_{t\to\infty} y_n(t) = \lim_{t\to\infty} \dot{y}_n(t) = 0$ for all n. If we solve (3) using the Ansatz $y_n(t) = \xi\, e^{\lambda t + in\theta}$, $\xi, \lambda \in \mathbb{C}^2$, $\theta \in \mathbb{R}$, we obtain the characteristic equation

$$\lambda^2 = \sum_{k=1}^{K} \alpha_k (e^{ik\theta} - 1) + \lambda \sum_{k=0}^{K} \beta_k e^{ik\theta}. \quad (4)$$

H is linearly stable if the non nil roots of the characteristic equation have strictly negative real parts.

2.2 Linear stability condition

The characteristic equation is the complex polynomial equation with coefficients $(\nu_\theta, \mu_\theta, \sigma_\theta, \rho_\theta) \in \mathbb{R}^4$

$$\lambda^2 + w_\theta \lambda + z_\theta = 0, \quad w_\theta = \mu_\theta + i\sigma_\theta, \quad z_\theta = \nu_\theta + i\rho_\theta \quad (5)$$

with $\mu_\theta = -\sum_{k=0}^{K} \beta_k c_{k\theta}$, $\nu_\theta = \sum_{k=1}^{K} \alpha_k (1 - c_{k\theta})$, $\sigma_\theta = -\sum_{k=1}^{K} \beta_k s_{k\theta}$, $\rho_\theta = -\sum_{k=1}^{K} \alpha_k s_{k\theta}$, using the notations $c_x = \cos x$ and $s_x = \sin x$.

The sufficient and necessary conditions for that a polynomial with complex coefficients have all its zeros in the half-plane $\Re(\lambda) < 0$ are given in [4, Th. 3.2]. The results are a generalization of the so-called Hurwitz conditions for polynomials with real coefficients. They are here $\sum_{k=0}^{K} \beta_k < 0$ and

$$\mu_\theta > 0, \quad \mu_\theta(\nu_\theta \mu_\theta + \rho_\theta \sigma_\theta) - \rho_\theta^2 > 0, \quad \theta \in]0, \pi]. \quad (6)$$

The condition is general and can be rediscovered in [13] with a model with one predecessor, or in [10] with the multi-anticipative optimal velocity model.

3. DISTANCE BASED MODELS

Many pedestrian dynamics models continuous in space are based on the superposition of a positive term to the desired speed and a negative repulsive one with the predecessors (see for instance [8, 5, 7])

$$\ddot{x}_n(t) = \frac{1}{\tau}(v_0 - \dot{x}_n(t)) - \sum_{k=1}^{K} f\left(x_{n+k}(t) - x_n(t)\right), \quad (7)$$

with $v_0, \tau > 0$ and f a differentiable, positive, decreasing function on $\mathbb{R}^+$. Here, the repulsive force f solely depends on the spacing.

With this model class, for a given mean spacing d, the equilibrium speed is $v = v_0 - \tau \sum_{k=1}^{K} f(kd)$. The speed v depends on v_0, K, d, τ and $f(.)$ parameters. The first linear stability condition (6) is here $-1/\tau < 0$. It is always true and implies the preliminary assumption. The second condition (6) is

$$-\frac{1}{\tau^2} \sum_{k=1}^{K} f'(kd)\,(1 - c_{k\theta}) - \left(\sum_{k=1}^{K} f'(kd) s_{k\theta} \right)^2 > 0. \quad (8)$$

Note that $f'(d) \leq 0$ for all d and thus the first term is positive and that the condition does not depend on v. The stability occurs for a relaxation time τ small enough. More precisely the homogeneous configurations are stable if and only if

$$0 < \tau < \tau_K = \inf_{\theta \in]0,\pi]} \tau_K^{(\theta)},$$
$$\text{with} \quad \tau_K^{(\theta)} = \left(\frac{-\sum_{k=1}^{K} f'(kd)\,(1 - c_{k\theta})}{\left(\sum_{k=1}^{K} f'(kd) s_{k\theta} \right)^2} \right)^{1/2}. \quad (9)$$

We have $\lim_{x\to\infty} f(x) = f(y) - \int_y^\infty |f'(u)|\ \mathrm{d}u = 0$ for all $y > 0$. This implies $\int_y^\infty |f'(u)|\ \mathrm{d}u < \infty$ since for all $y > 0$, $f(y) < \infty$. Using the Cauchy criteria and changing the variable, one then obtains

$$\sum_{k=1}^{\infty} |f'(dk)| < \infty, \quad d > 0. \quad (10)$$

This proves the absolute convergence of $\tau_K^{(\theta)}$ and τ_K, and means that the stability condition at the limit $K \to \infty$ may be approximated for an finite value of K. It exist with this model class an intrinsic interaction range. The value of the range depends on the convergence speed of the series $\sum_k |f'(dk)|$. This point will be further investigated using well-know repulsive forces f.

3.1 Exponential and inverse models

Let firstly consider the exponential repulsive force with parameters $A, B > 0$ into (7)

$$f(d) = Ae^{-d/B}, \qquad f'(d) = -A/Be^{-d/B}. \quad (11)$$

This force is used in the social force model [8]. Because of the use of exponential decreasing, the interaction model is short range. We use the uni-dimensional parameter $u = d/B > 0$ and critical relaxation time

$$\tilde{\tau}_K^{(\theta)} = \sqrt{\frac{A}{B}} \tau_K^{(\theta)}. \quad (12)$$

We have with the exponential repulsive force (11) using (9)

$$\tilde{\tau}_K^{(\theta)}(u) = \left(\frac{\sum_{k=1}^{K} e^{-ku}\,(1 - c_{k\theta})}{\left(\sum_{k=1}^{K} e^{-ku} s_{k\theta} \right)^2} \right)^{1/2}. \quad (13)$$

u is a shape parameter, while A and B are scale parameters for the stability.

The inverse repulsive force with parameters $A, B, q > 0$ is

$$f(d) = \frac{A}{(d/B)^q}, \qquad f'(d) = -\frac{qA/B}{(d/B)^{q+1}}. \quad (14)$$

This model is used in [5] with $q = 1$ and in [7] with $q = 2$. Here, the model can be short or long range depending on the value of q. It induces a polynomial convergence speed of f' to zero, slower than the exponential speed of the model (11). This suggests higher number of pedestrians in interaction K to stabilize the critical time τ_K. We have with this model the dimensionless critical relaxation time

$$\tilde{\tau}_K^{(\theta)}(u, q) = \left(\frac{u^{q+1}}{q} \frac{\sum_{k=1}^{K} (1 - c_{k\theta}) k^{-(q+1)}}{\left(\sum_{k=1}^{K} s_{k\theta} k^{-(q+1)} \right)^2} \right)^{1/2}. \quad (15)$$

Here again, only q is a shape parameter.

3.2 Stability condition

The uniform solution (2) is linearly stable for the distance based models (11) and (14) if the relaxation time τ is strictly less than critical time $\tau_K = \inf_\theta \tau_K(\theta)$ (or if $\sqrt{A/B}\tau < \tilde{\tau}_K$). Thus we have to calculate the minimum of the functions $\theta \mapsto \tilde{\tau}_K(\theta)$ to determine the stability condition. Yet, the signs of the derivative of these functions are hardly analytically extracted. We investigate it numerically.

The critical time (13) of the exponential model (11) is plotted as a function of θ in figure 1. Here, K varies from 1 to 25, and $u = 0.4$, 1 and 2.5. The $\tilde{\tau}_K^{(\theta)}$ are minimal at the limit $\theta \to 0$ for all K, *i.e.* $\tilde{\tau}_K = \lim_{\theta\to 0} \tilde{\tau}_K^{(\theta)}$ with the exponential force (11). Further numerical investigations (not shown here) confirm this observation.

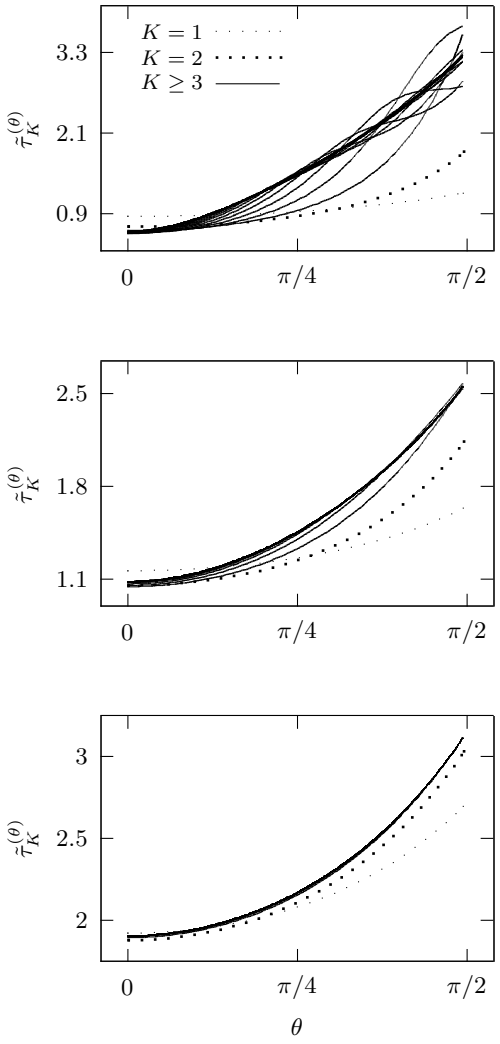

Figure 1: The $\tilde{\tau}_K^{(\theta)}$, $K = 1, \ldots, 25$, as a function of θ for the exponential model (11). From top to bottom $u = 0.4, 1, 2$.

The critical time (13) for the inverse model (14) is plotted as a function of θ in figure 2 with $q = 1$, 2 and 3. The $\tau_K^{(\theta)}$ are minimal for $\theta \to 0$ when K is low. For high values of K, the minimums of $\tau_K^{(\theta)}$ are reached for $\theta = \theta_{q,K} > 0$. Further results show that $\theta_{q,K}$ converge when K increases. Therefore the wave's lengths the more unstable have characteristic values with the inverse model, if K is large enough.

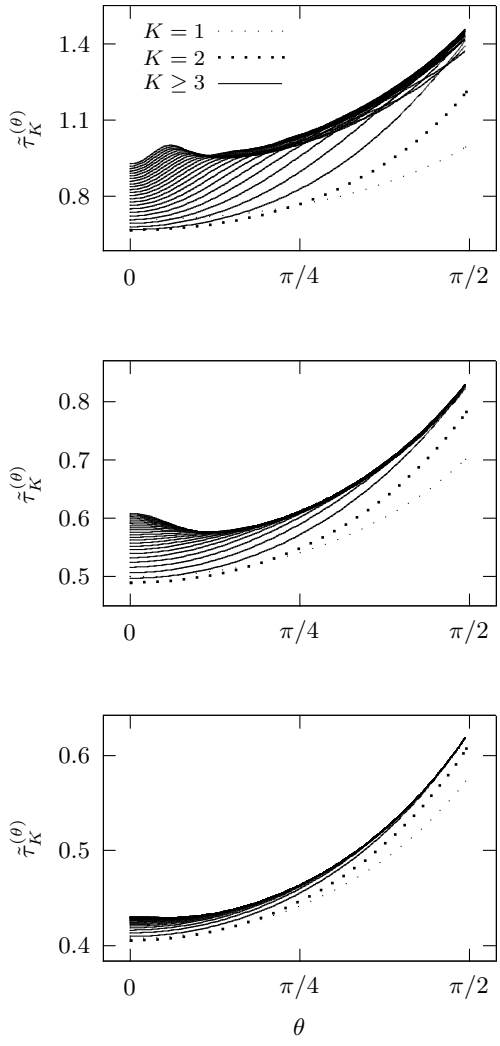

Figure 2: The $\tilde{\tau}_K^{(\theta)}$, $K = 1, \ldots, 25$, as a function of θ for the inverse model (14). From top to bottom $q = 1, 2, 3$; $u = 1$.

3.3 Stability function of K

The dimensionless critical time $\tilde{\tau}_K$ delimits the border of the linear stability of uniform solutions. The stability occurs if $\sqrt{A/B}\tau$ is strictly smaller than $\tilde{\tau}_K$ (see (9)).

The dimensionless function $K \mapsto \tilde{\tau}_K$ is plotted in figure 3 for the model (11), and in figure 4 for (14). One can observe for both models that the critical time τ_K converges to a constant value through a single damped oscillation. This non linear relation between K and the stability is surprising. Increasing the number of pedestrians in interaction firstly results as a decreasing of the stability (at least until $K = 2$). Then increasing K increase τ_K and so the stability. The convergence of τ_K is relatively smooth with the model (11).

One observes a brusque transition with the model (14), when the minimum is reached for the $\theta_{q,K}$. The form and speed of the damping of function $K \mapsto \tilde{\tau}_K$ depend on parameter u for the model (11), and on q for (14).

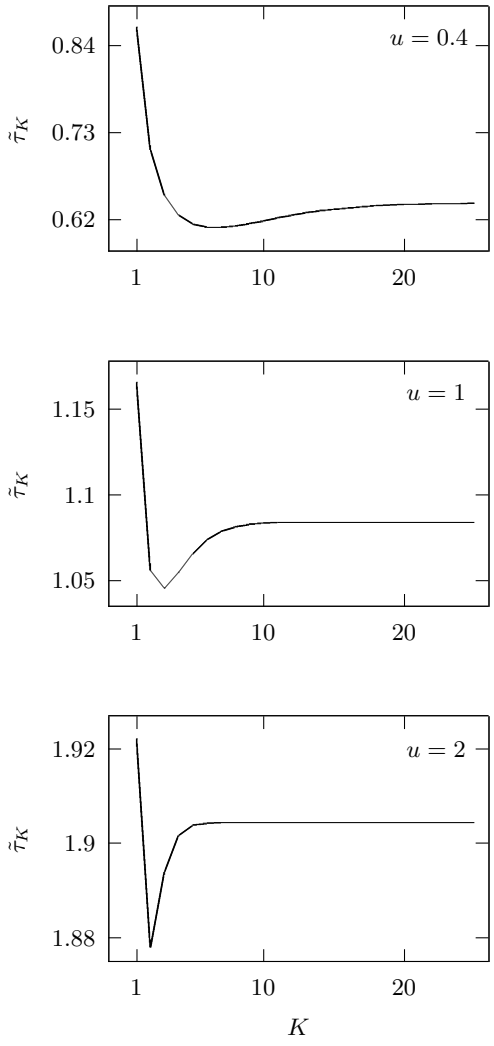

Figure 3: $\tilde{\tau}_K = \inf_\theta \tilde{\tau}_K^{(\theta)}$ **as a function of** K **for the exponential-distance model (11) with** $u = 0.4,\ 1,\ 2$**.**

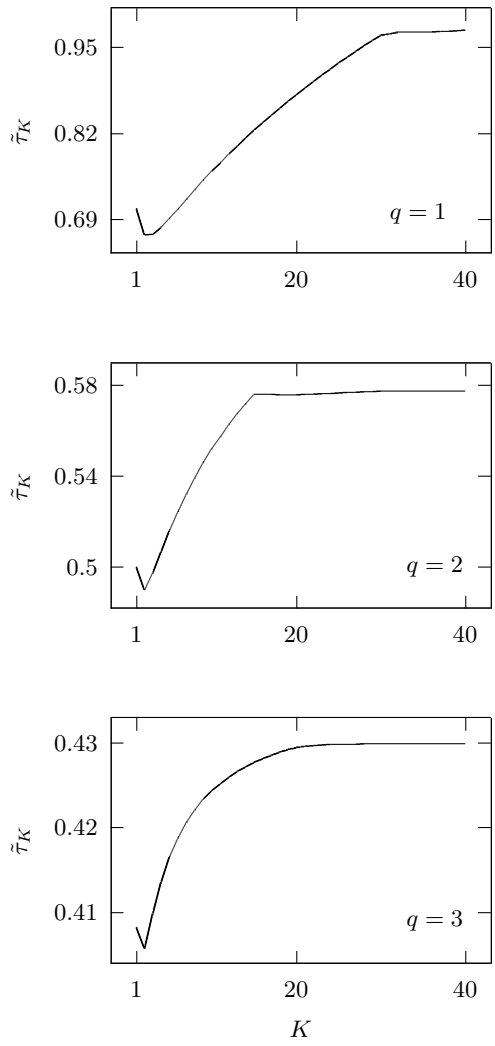

Figure 4: $\tilde{\tau}_K = \inf_\theta \tilde{\tau}_K^{(\theta)}$ **as a function of** K **for the inverse model (14) with** $q = 1,\ 2,\ 3$**;** $u = 1$**.**

3.4 Proportion of variation

The figures 3 and 4 show damping oscillations of $\tilde{\tau}_K$ as K increases. Here, we investigate the amplitude of the oscillation. For that purpose, we introduce the proportion

$$\varphi = 1 - \frac{\min_K \tilde{\tau}_K}{\max_K \tilde{\tau}_K} = 1 - \frac{\min_K \tau_K}{\max_K \tau_K}, \qquad (16)$$

that is the same for the initial and dimensionless critical time τ_K and $\tilde{\tau}_K$.

The proportion of variation $\varphi \in [0, 1]$ describes how the models depend on the number K. For $\varphi \approx 0$, the model poorly depends on the interaction range, i.e. the stability condition as $K \to \infty$ is well approximated using few predecessors (K small), and oppositely for $\varphi \approx 1$. For both models (11) and (14), φ does not depend on A and B. It depends on u for the exponential model (11), while it depends on q for the inverse model (14), but not on u.

In figure 5, the proportion of variation φ is plotted as a function of u for the model (11) (top plot), and as a function of q for the model (14) (bottom plot). φ tends to zero as the dimensionless mean spacing u increases within model (11). This means that for low density level, the stability condition at the limit $K \to \infty$ can be well estimated using few predecessors. For high densities, the variability of $\tilde{\tau}_K$ is more important. The same phenomena occurs as q increases within model (14). For short range model where q is high, few predecessor in interaction are sufficient to estimate the stability condition as $K \to \infty$ and oppositely. Surprisingly, the proportion of variation does not depend on the density level with the inverse model. This changes in the case when the distance spacing d is taken as $d - \ell$ to take into account the size $\ell > 0$ of the pedestrians.

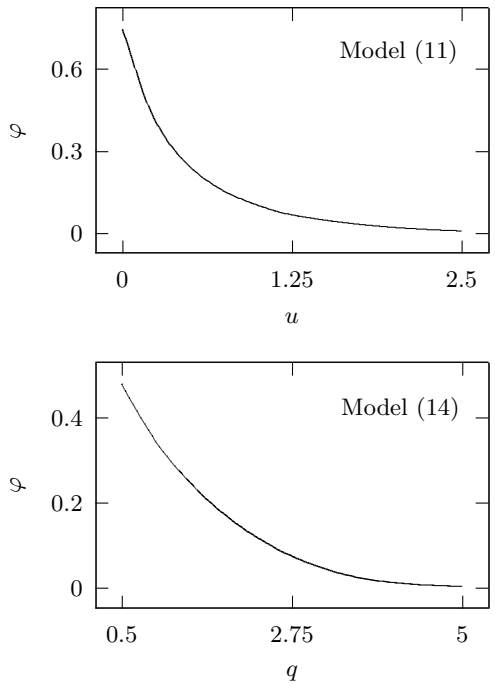

Figure 5: Proportion φ of variation of τ_K as K increases. Left, function of u, model (11). Right, function of q, model (14).

3.5 Stability function of the parameters

The function $\tilde{\tau}_K$ depends on the parameter u for the model (11), and on (u, q) for (14). For the model (11), the function $u \mapsto \tilde{\tau}_K(u)$ increases to infinity as u increases. This means that the stability increase as the distance spacing increases, for any K. One has explicitly

$$\frac{\partial \tilde{\tau}_K^{(\theta)}}{\partial u}(u) = \frac{\tilde{\tau}_K^{(\theta)}(u)}{2} g_K^{(\theta)}(u) > 0 \tag{17}$$

with $g_K^{(\theta)}(u) = -\frac{\sum_{k=1}^K k\, e^{-uk}(1-c_{k\theta})}{\sum_{k=1}^K e^{-uk}(1-c_{k\theta})} + \frac{2\sum_{k=1}^K k\, e^{-uk} s_{k\theta}}{\sum_{k=1}^K e^{-uk} s_{k\theta}}$.

We have $g_1^{(\theta)}(u) = 1$ for all u, while $\lim_u g_K^{(\theta)}(u) = 1$ for all u and all $K > 1$.

In top figure 6, the increasing critical time $\tilde{\tau}_K(u)$ at the limit $K \to \infty$ are compare to the time $\tilde{\tau}_1(u)$ for $K = 1$. One has $\lim_K \tilde{\tau}_K(u) < \tilde{\tau}_1(u)$ for all u, while, as expected since the proportion of variation tends to zero, $\lim_u \tilde{\tau}_1(u) = \lim_u \tilde{\tau}_K(u)$ for any K.

For the model (14), the function $u \mapsto \tilde{\tau}_K^{(\theta)}(u, q)$ also increases as u increases since

$$\frac{\partial \tilde{\tau}_K^{(\theta)}}{\partial u}(u, q) = \frac{q+1}{u} \tilde{\tau}_K^{(\theta)}(u, q) > 0. \tag{18}$$

The relation $q \mapsto \tilde{\tau}_K^{(\theta)}(u, q)$ is more complicated. For $u < 1$, the function decreases to zero as q increases. This means that stability never holds for any τ for enough high q. For $u = 1$, $\tilde{\tau}_K^{(\theta)}(1, q)$ tends to a constant value, while, for $u > 1$, the relation, successively decreasing and increasing, admits a minimum for certain q depending on u. One has

$$\frac{\partial \tilde{\tau}_K^{(\theta)}}{\partial q}(u, q) = \frac{\tilde{\tau}_K^{(\theta)}(u, q)}{2} \left(\ln u - \frac{1}{q} + h_K^{(\theta)}(q) \right), \tag{19}$$

$h_K^{(\theta)}(q) = -\frac{\sum_{k=1}^K \ln k\, k^{-(q+1)}(1-c_{k\theta})}{\sum_{k=1}^K k^{-(q+1)}(1-c_{k\theta})} + \frac{2\sum_{k=1}^K \ln k\, k^{-(q+1)} s_{k\theta}}{\sum_{k=1}^K k^{-(q+1)} s_{k\theta}}$.

For $K = 1$, $h_1^{(\theta)}(q) = 0$ for all q, and the sign of $\partial \tilde{\tau}_1^{(\theta)}/\partial q > 0$ is the sign of $\ln u - 1/q$. It is negative for all q if $u < 1$. If $u > 1$, $\partial \tilde{\tau}_1^{(\theta)}/\partial q < 0$ for $q < 1/\ln u$, and $\partial \tilde{\tau}_1^{(\theta)}/\partial q > 0$ for $q > 1/\ln u$. The $\tilde{\tau}_1^{(\theta)}(u, q)$ are minimum for $q = 1/\ln u$. Comparable properties are obtained for $K > 1$. One has $-1/q + h_K^{(\theta)}(q) \to -\infty$ as $q \to 0$, $\partial \tilde{\tau}_K^{(\theta)}/\partial q$ is firstly negative, and it is of the sign of $\ln u$ as q increases since $-1/q + h_K^{(\theta)}(q) \to 0$ as $q \to \infty$.

The critical time $\tilde{\tau}_K(u, q)$ at the limit $K \to \infty$ is compared to $\tilde{\tau}_1(u, q)$, for $u = 0.4$ and $u = 2$, and as a function of q in bottom figure (6). Here $\tilde{\tau}_1(u, q) < \lim_K \tilde{\tau}_K(u, q)$ for all u, q, while, as expected, $\lim_q \tilde{\tau}_1(u, q) = \lim_q \tilde{\tau}_K(u, q)$ for any K and u.

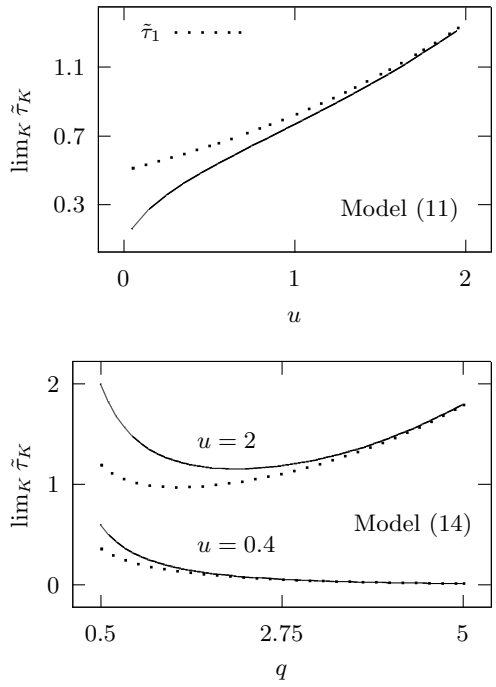

Figure 6: Dimensionless critical relaxation time $\tilde{\tau}_K = \inf_\theta \tilde{\tau}_K^{(\theta)}$ for $K = 1$ (dotted lines), and at the limit $K \to \infty$ (continuous lines). Top, function of u, model (11). Bottom, function of q, model (14).

3.6 Optimal velocity model

The multi-anticipative optimal velocity model with $K \geq 1$ predecessors in interaction [10] is

$$\ddot{x}_n(t) = \sum_{k=1}^K a_k \left\{ V\left(\frac{1}{k}(x_{n+k}(t) - x_n(t)) \right) - \dot{x}_n(t) \right\}. \tag{20}$$

Here $(a_k) \in \mathbb{R}_+^K$. With this model, the equilibrium speed v corresponding to the mean spacing d is $v = V(d)$. The first

condition (6) is $\sum_{k=1}^{K} a_k > 0$. It is always true and implies the preliminary assumption. The second condition (6) is, after rearranging

$$0 < V' < \frac{\left(\sum_{k=1}^{K} a_k\right)^2 \sum_{k=1}^{K} \frac{a_k}{k}\left(1 - c_{k\theta}\right)}{\left(\sum_{k=1}^{K} \frac{a_k}{k} s_{k\theta}\right)^2} \qquad (21)$$

(see [10, Eq. (14)]).

Note that the case $K = 1$ corresponds to the well know Optimal Velocity model [1]. For this model, the condition is $V'(d) < a_1/(1 + c_\theta)$. Since $1/(1 + c_\theta) > 1/2$, the condition holds for all $\theta \in]0, 2\pi[$ if $V'(d) < a_1/2$ (see [1]).

If we assume that $1/a_k = \tau k^q$ with $\tau > 0$ and $q \geq 0$ a parameter calibrating the interaction range (in a similar way than with the inverse model (14)), one obtains the condition

$$0 < \tau V' < \frac{\left(\sum_{k=1}^{K} k^{-q}\right)^2 \sum_{k=1}^{K} \left(1 - c_{k\theta}\right) k^{-(q+1)}}{\left(\sum_{k=1}^{K} s_{k\theta} k^{-(q+1)}\right)^2} =: \tilde{\tau}_K^{(\theta)}. \qquad (22)$$

The mean spacing has only a role through the derivative of the optimal speed function that is a scale parameter. Only q is a shape parameter. The expression of $\tilde{\tau}_K^{(\theta)}$ is comparable to the one of the inverse model (14), see (15). Here, the time is proportional to the square of $\sum_k k^{-q}$ and converges if and only if $q > 1$. In this case, the forms of the functions $\theta \mapsto \tilde{\tau}_K^{(\theta)}$ are comparable to the ones obtained with the inverse model (14) (see in figure 2). The functions $K \mapsto \tilde{\tau}_K = \inf_\theta \tilde{\tau}_K^{(\theta)}$ are also comparable with the difference that the functions are always increasing, with no damped oscillation. With the OV model (20), increasing the number of predecessors in interaction results in an increase of the stability, for any $V'(d) > 0$.

The proportion of variation of the critical time $\tilde{\tau}_K$ as K varies, denoted φ, is not defined when $q \leq 1$ since the $\tilde{\tau}_K$ diverges (it could be equal to 1). For $q > 1$, the proportion tends to zero as q increases. As expected, and as the inverse model (14), see in top figure 5, the influence of K decreases as the model becomes short range (i.e. as q increases). The critical time does not depends on q for $K = 1$. For any $K > 1$, the times decreases as the q increases. The stability is negatively influenced by the range q. The constant minimal value for $K = 1$ corresponds here to the limit as q increases of the critical time $\tilde{\tau}_K$ for all $K > 1$ ($\lim_q \tilde{\tau}_K(q) = \tilde{\tau}_1 > 0$, see in bottom figure 7). This means that, oppositely to the inverse model (14) with $u < 1$, the OV model can remain stable at the limit $q \to \infty$, for any K.

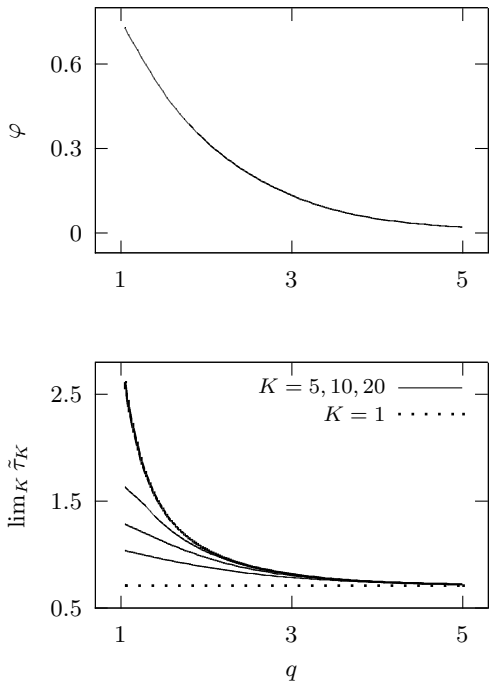

Figure 7: Top, the proportion of variation of the critical time with the OV model (20). Bottom dimensionless critical time for $K = 1, 5, 10, 20$ and at the limit $K \to \infty$ (thick line).

4. SUMMARY AND CONCLUSION

Linear stability conditions of uniform solutions are calculated for a second order pursuit model, with $K \geq 1$ predecessor in interaction. The framework is general and includes many models used in pedestrian dynamics as well as in road traffic flow. The conditions are explored using particular pedestrian models for which the dynamics are the sum of an acceleration term to the desired speed, and a repulsive one with the predecessors, or with the well-known optimal velocity car-following model. For the pedestrian models, the acceleration to the desired speed is calculated using a relaxation process, while the repulsion is a sum over the predecessors in the interaction. The desired speed is a function of the spacing with the optimal velocity model. Within the different forms tested, the stability occurs for a small enough relaxation time τ, smaller than a critical time τ_K.

When the repulsive force depends solely on the distance spacing, the critical time converges as K increases, with a damped oscillation. The role of the parameter K on the stability threshold is not negligible when the repulsive term does not decrease sufficiently fast as the distance spacing d increases (i.e. force $f(d) \propto e^{cd}$ or $1/d^q$ with low c, q). On the opposite, the proportion of variation of τ_K as K varies is low when the interaction range model are short (i.e. high c or q parameters). Comparable properties are obtained within the car-following optimal velocity model if $q > 1$.

The number of predecessors in interaction in the pursuit modeling modify the stability conditions. As expected, the influence of the parameter depends on the form of the model. It exists finite interaction thresholds for the stability within distance based models. In a separate paper we will show that it is generally not the case when the models also depends on the speeds. The overview developed here could be useful regarding jam waves formation, for analysis or validation of pedestrian as well as car-following models.

5. REFERENCES

[1] M. Bando, K. Hasebe, A. Nakayama, A. Shibata, and Y. Sugiyama. Dynamical model of traffic congestion and numerical simulation. *Phys. Rev. E*, 51(2):1035–1042, 1995.

[2] S. Bexelius. A extended model for car-following. *Transp. Res.*, 2(1):13–21, 1968.

[3] D. Chowdhury, L. Santen, and A. Schadschneider. Statistical physics of vehicular traffic and some related systems. *Phys. Rep.*, 329(4-6):199–329, 2000.

[4] E. Frank. On the zeros of polynomials with complex coefficients. *Bull. Amer. Math. Soc.*, 52(2):144–157, 1946.

[5] R.Y. Guo, S.C. Wong, H.-J. Huang, and W.H.K. Lam. A micoscopic pedestrian-simulation model and its application to intersecting flows. *Physica A*, 389(3):515–526, 2010.

[6] D Helbing. Traffic and related self-driven many-particle systems. *Phys. Mod. Phys.*, 73(4):1067–1141, 2001.

[7] D. Helbing, I.J. Farkas, and T. Vicsek. Freezing by heating in a driven mesoscopic system. *Phys. Rev. Lett.*, 84(6):1240–1243, 2000.

[8] D. Helbing and P. Molnár. Social force model for pedestrian dynamics. *Phys. Rev. E*, 51(5):4282–4286, 1995.

[9] S. Hoogendoorn, S. Ossen, and M. Schreuder. Empirics of multianticipative car-following behavior. In *Transportation Research Record*, number 1965, pages 112–120, 2006.

[10] H. Lenz, C.K. Wagner, and R. Sollacher. Multi-anticipative car-following model. *Eur. Phys. J. B*, 7(2):331–335, 1999.

[11] G. Orosz, R.E. Wilson, and G. Stepan. Traffic jams : dynamics and control. *Proc. R. Soc. A*, 368(1957):4455–4479, 2010.

[12] A. Tordeux, S. Lassarre, and M. Roussignol. An adaptive time gap car-following model. *Transp. Res. B*, 44(8-9):1115–1131, 2010.

[13] A. Tordeux, M. Roussignol, and S. Lassarre. Linear stability analysis of fisrt-order delayed car-following models on a ring. *Phys. Rev. E*, 86(3):036207, 2012.

[14] M. Treiber and A. Kesting. *Traffic Flow Dynamics*. Springer, Berlin, 2013.

[15] M. Treiber, A. Kesting, and D. Helbing. Delays, inaccuracies and anticipation in microscopic traffic models. *Physica A*, 360(1):71–88, 2006.